International Journal of PSYCHOLOGICAL RESEARCH

RESEARCH ARTICLE

Vol 17, N° 2
https://revistas.usb.edu.co/index.php/IJPR
ISSN 2011-2084
E-ISSN 2011-7922

Unveiling Visual Physiology and Steady-State Evoked Potentials using Low-Cost and Transferable Electroencephalography for Evaluating Neuronal Activation

Presentando la fisiología visual y los potenciales evocados en estado estable utilizando electroencefalografía de bajo costo y transferible para evaluar la activación neuronal

Verónica Henao Isaza[1,2⋆], Valeria Cadavid Castro[1,2], Eliana Salas Villa[1,2], Santiago Gonzalez Cuartas[1,2], John Fredy Ochoa[1].

[1] *Grupo Neuropsicología y Conducta (GRUNECO), Facultad de Medicina, Universidad de Antioquia, Calle 67 N 53 108, Medellín, 050001, Antioquia, Colombia.*

[2] *Semillero de Investigación Neurociencias Computacionales (NeuroCo), Facultad de Medicina & Facultad de Ingeniería, Universidad de Antioquia, Calle 67 N 53 108, Medellín, Colombia, Medellín, 050001, Antioquia, Colombia.*

Abstract.
Purpose. The ability to see and process images depends on the function of the eyes and the processing of visual information by neurons in the cerebral cortex, something that could be measured through electroencephalography (EEG). Although the EEG is used to evaluate visual pathways in children and demyelination diseases, the limited utilization of brain recording techniques in other applications like therapy is primarily due to budget constraints. The goal of this paper is to demonstrate results from studying brain aspects of vision, utilizing measurements based on oscillatory activity analysis, low-cost, portable equipment, and a processing pipeline relying on Python's open-source libraries. These studies involve healthy subjects who wear glasses to assess changes in visual perception. **Methods.** First, electroencephalographic signals were recorded while the subjects observed a visually standardized stimulus. The signals were processed and filtered to reduce artifacts, and the power spectral density (PSD) was calculated to observe the presence of steady-state visual potentials (VEP) to confirm the capture of neuronal activation to the visual stimulus. **Results.** It was possible to establish a difference between subjects wearing and not wearing their glasses, allowing validation that the information acquired with the transferable equipment is adequate for the analysis of neuronal activity related to visual processing, opening the possibility to be used in future studies in therapy. **Conclusion.** This study contributes to the development of cost-effective and portable EEG solutions for visual system analysis. It demonstrates the potential for applying transferable EEG devices in clinical settings and highlights the importance of tailored visual stimuli for reliable neural activation.

Resumen.
Propósito. La capacidad de ver y procesar imágenes depende de la función de los ojos y del procesamiento de la información visual por parte de las neuronas en la corteza cerebral, algo que podría medirse mediante electroencefalografía (EEG). Aunque el EEG se utiliza para evaluar las vías visuales en niños y enfermedades desmielinizantes, la utilización limitada de técnicas de grabación cerebral en otras aplicaciones como la terapia se debe principalmente a restricciones presupuestarias. El objetivo de este artículo es demostrar resultados del estudio de aspectos cerebrales de la visión, utilizando mediciones basadas en el análisis de actividad oscilatoria, equipos de bajo costo y portátiles, y un flujo de procesamiento basado en las bibliotecas de código abierto de Python. Estos estudios involucran a sujetos sanos que usan gafas para evaluar cambios en la percepción visual. **Métodos.** Primero, se registraron señales electroencefalográficas mientras los sujetos observaban un estímulo visual estandarizado. Las señales fueron procesadas y filtradas para reducir artefactos, y se calculó la densidad espectral de potencia (PSD) para observar la presencia de potenciales visuales en estado estable (VEP) y confirmar la captura de la activación neuronal ante el estímulo visual. **Resultados.** Fue posible establecer una diferencia entre los sujetos que llevaban y no llevaban sus gafas, permitiendo validar que la información adquirida con el equipo transferible es adecuada para el análisis de la actividad neuronal relacionada con el procesamiento visual, abriendo la posibilidad de ser utilizada en estudios futuros en terapia. **Conclusión.** Este estudio contribuye al desarrollo de soluciones de EEG de bajo costo y portátiles para el análisis del sistema visual. Demuestra el potencial de aplicar dispositivos de EEG transferibles en entornos clínicos y resalta la importancia de estímulos visuales adaptados para una activación neural confiable.

Keywords.
Electroencephalography, Processing, SSVEP, Stimulation, Transferable, Visual Function.
Palabras Clave.
Electroencefalografía, procesamiento, SSVEP, estimulación, transferible, función visual.

OPEN ACCESS

Manuscript received: 30-10-2023
Revised: 19-05-2024
Accepted: 01-08-2024

⋆**Corresponding author**:
Verónica Henao Isaza
Email: veronica.henaoi@udea.edu.co

Declaration of data availability: All relevant data are within the article, as well as the information support files.

Conflict of interests: The authors have declared that there is no conflict of interest.

How to Cite:
Henao Isaza, V., Cadavid Castro, V., Salas Villa, E., Gonzalez Cuartas, S., & Ochoa, J. F. (2024). Unveiling Visual Physiology and Steady-State Evoked Potentials using Low-Cost and Transferable Electroencephalography for Evaluating Neuronal Activation. *International Journal of Psychological Research*, *17*(2), 25–35. https://doi.org/10.21500/20112084.7299

1. Introduction

Vision loss is one of the most debilitating sensory deficits for humans, as we rely heavily on our sense of sight to gather information from the external environment. This becomes more apparent when considering the percentage of the cerebral cortex allocated to our visual system, which imposes a high risk of visual loss when brain damage occurs.

Electroencephalography (EEG) signals are recorded noninvasively through electrodes placed on the scalp and have a high temporal resolution, making it one of the most widely used recording modalities to study brain activity (Orban et al., 2022). EEG measures the electrical activity of the brain caused by the flow of electrical currents during synaptic excitations and inhibition of dendrites in neurons (Beniczky et al., 2020; Brienza et al., 2019). EEG research is useful in the diagnosis and rehabilitation of the cognitive problems of individual head injury (Alouani et al., 2022; Kadri et al., 2022), and visual evoked potentials (VEP) have shown information about the functional status of the visual system (Sanchez-Lopez et al., 2019). Other studies have also used these potentials to characterize vision functions in children and adults and have reported objective measures to support clinical evaluations in healthy subjects and visually impaired patients (Bach et al., 2019; Hemptinne et al., 2019; Kiiski et al., 2016; Sahel et al., 2021; Sarzaeim et al., 2022; Zheng et al., 2019). However, although VEPs are measurements that offer valuable information on amplitude, latency, and spectral characteristics, some of them are sensitive to external factors such as the type of monitor, signal acquisition system, ambient light, etc. (Fox et al., 2014). It is important to analyze EEG measurements that can be sensitive indicators of pathology (Zhong et al., 2023) and allow the use of transferable equipment that facilitates implementation in clinical settings. VEPs are the most widely used technique to explore the visual cortex since they allow the exploration of basic visual neurophysiology and the diagnosis of various optical and neurological pathologies. There are two forms for VEPs: VEP transient and VEP stationary or Steady State VEP (SSVEP). Transient VEPs (TVEPs) occur when stimuli are presented at a slow rate (below 4 Hz), allowing the stimulus-evoked brain activity to return to baseline before the next stimulus is delivered (Nicolas-Alonso et al., 2012; Sanchez-Lopez et al., 2019). Some studies have carried out treatments for multiple sclerosis (MS) and optic neuritis, showing significant results with P100 in rehabilitation treatments (Kiiski et al., 2016; Marcar et al., 2018). It is more common to use steady-state VEP (SSVEP) to analyze neuro-ophthalmological diseases (Sanchez-Lopez et al., 2019), considering the SSVEP as a solid method to study visual perception, spatial and selective attention, cognitive fatigue, and working memory (Mora-Cortes et al., 2018). Repetitive (or flickering) visual stimuli occur at high frequency (usually 6 to 20 Hz), as proposed by Lantz et al. (2021), causing a continuous and constant sequence of oscillatory potential changes that arise primarily in the visual cortex. This stimulation is fast enough to prevent evoked neural activity from returning to baseline. SSVEPs reflect high-propagation properties (i.e., a mix of local and widely distributed time sources), are less sensitive to different types of artifacts, require much less time to acquire data, and have a higher signal-to-noise ratio (SNR) than the TVEP (Norcia et al., 2015; Sanchez-Lopez et al., 2019). In addition, other SSVEPs have made it possible to measure acuity and contrast sensitivity (Almoqbel et al., 2017; Baker et al., 2015). Therefore, these potentials are a useful tool to characterize the visual system differences, and they are even observed when evaluating the visual system using filters or lenses, or when performing monocular and binocular tasks (Richard et al., 2018). This study focuses specifically on visual physiology and steady-state evoked potentials and aims to demonstrate the efficacy of a portable EEG device, and the OpenBCI acquisition device used in previous work (Cadavid et al., 2021; Ortega et al., 2019), to capture visually evoked potentials that differentiate stimulus perception in individuals with corrected-to-normal vision. The research includes the development of a protocol that combines visual testing and EEG measurements. By analyzing the acquired EEG signals, the study provides recommendations for procedures in stimulation, EEG recording and processing, and data analysis. The results consistently showed that neurons were activated in all cases, confirming that the portable device is effective for studying the brain. This research intends to provide helpful suggestions for recording SSVEP using OpenBCI, which could create common ways to do things like (a) deciding how to make the brain respond, (b) recording and looking at brain activity, and (c) performing data analysis. Furthermore, this study also reveals differences in the effects of wearing glasses, which adds more insight to using SSVEP to study how our visual system works. The following sections describe the current methodology for detecting neural activation, starting with the selection of the population of interest. Next, the tools for developing the experimental stimulation tasks and the subject's position during stimulation are developed. Then, the data acquisition protocols and the different preprocessing steps (e.g., EEG acquisition and processing, reference, artifact removal, wavelet, and FIR filtering) are considered. After that, the recorded EEG signals in which the VEP is present are analyzed by observing the power spectral density at the stimulation frequency, and a survey is conducted to assess the subject's comfort level. Finally, the results obtained using the signal-to-noise ratio (SNR) and Welch's method are presented and discussed to draw conclusions.

2. Methods

2.1 Subjects

23 adult volunteers were evaluated, 13 women and 10 men, aged between 18 and 60 years with a mean age of 25.04 ± 9.0 years. This group comprised individuals who rely on glasses for their daily activities. The aim was to assess potential variations in visual perception among participants when conducting experiments with and without glasses.

Additionally, participants were required to have no history of epilepsy due to the potential risk of certain types of visual stimuli triggering seizures in individuals with this condition.

Ethical approval declarations. All participants were from Medellín, Colombia, and the surrounding area, and signed an informed consent form approved by the Ethics Committee of the University Research Center of Universidad de Antioqia (Acta 18-59-828).

Participants were recruited through telephone calls, an enrollment form, and e-mail. Personal and demographic data, such as age, sex, and whether they suffered from epilepsy, were previously recorded. At the end of the recording, each subject was given a satisfaction test survey using the Google form, where comfort during the test, perception of the stimuli, and additional suggestions were recorded.

2.2 Stimulation Conditions

The stimulus was created using the Python 2.7 programming language, Psychopy3 experiment creation software, and the OpenDesigner tool, and was presented on a Samsung SyncMaster 2243LNX display. During the experiment, subjects kept their heads on a stand to maintain a viewing distance of 1 meter, the stimulus was displayed for binocular vision, and all participants were guided to remain comfortably seated while attentively observing the stimulus, avoiding movement during recording. The visual stimulus employed was Vernier acuity. This involved switching between two patterns: a regular linear grating and a grating with a Vernier displacement of 15 arcminutes. These states alternated at a rate of 5 Hz, and the entire stimulation lasted for 30 seconds. The operational setup can be observed in Figure 1. This stimulus was selected because it activates the visual cortex and allows obtaining the visual acuity from the EEG measurement (Tan et al., 2018; Zheng et al., 2020), and the selected stimulation frequency has a greater amplitude compared to other frequencies and provides greater comfort during stimulation (O'Hare, 2017).

2.3 EEG Acquisition

The acquisition of brain activity was performed via EEG from eight electrodes (FCz, Oz, O1, O2, PO7, PO8, PO3, and PO4) placed according to the 10-10 system (Nuwer, 2018). The specific placement of these electrodes is illustrated in Figure 2. The data were recorded directly from a code generated in Python language and the data was acquired via Bluetooth from the OpenBCI device card at a sampling rate of 250 Hz.

Figure 1

Schematic Representation of the Stimulus used in the Experiment

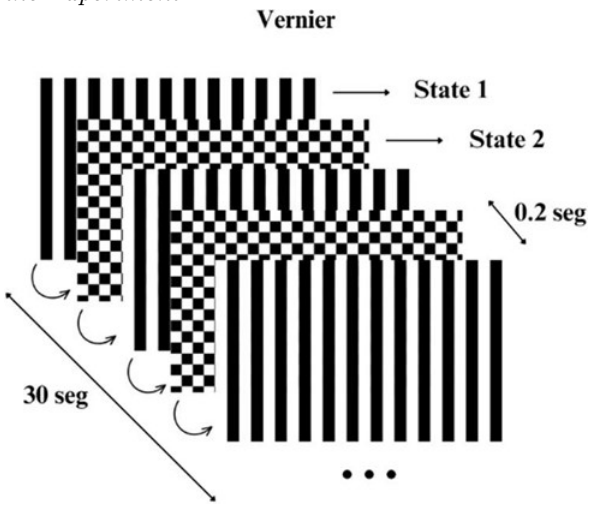

Note. The stimulus oscillates at a frequency of 5 Hz, resulting in a switching time between states 1 and 2 of .2 seconds. Source: authors.

Figure 2

Schematic Representation of the Electrode Setup Utilized during Experimentation

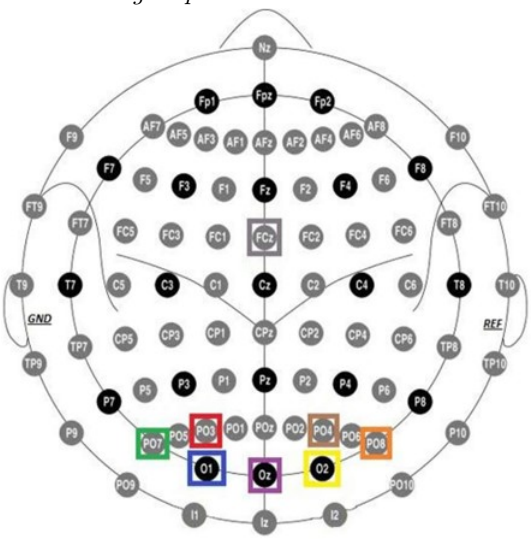

Note. The electrodes are positioned over the occipital area, targeting the visual cortex, constituting approximately 5% of the total electrode array. Source: authors.

Signal acquisition was only performed after the following procedures were completed for the EEG device: calibration of the channel impedance, ensuring that the contact impedances of the EEG electrodes were kept below 30 kΩ, connection of the ground and reference

channel sockets to the common and reference ground, respectively, located on the earlobes. Finally, verification that the signals captured by the electrodes were stable.

Signals were recorded for each subject in the present study at rest with eyes closed and at rest with eyes open, both for 5 minutes. Finally, signals were recorded for each subject under stimulation conditions, as illustrated in Figure 3. The stimulation was measured both with and without glasses to observe differences in EEG responses to the same visual stimulus.

Figure 3

Sequence of the Experimental Task

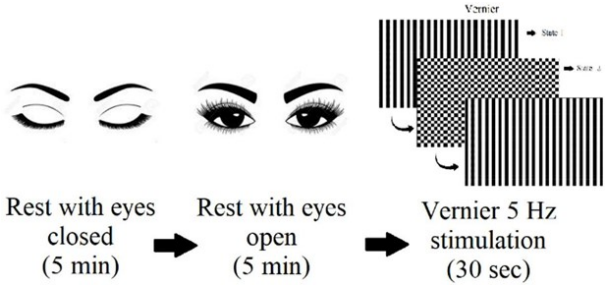

Note. This diagram outlines the sequence of the experimental task. It begins with a 5-minute rest period with eyes closed, followed by a 5-minute rest period with eyes open. The task concludes with a 30-second stimulation using a 5 Hz Vernier pattern while the subject's eyes remain open. This sequence aims to establish baseline EEG activity with and without visual input, and then measure the response to specific visual stimulation. Source: authors.

2.4 EEG Processing

The data processing flow is shown in Figure 4. EEG signals obtained were loaded and processed in Python 3.0 using the Google Collaboratory tool.

As a first step in the preprocessing of the different signals obtained, a re-referencing was carried out by using as reference the signal of the FCz electrode (see Figure 2), located at the medial zone of the coronal suture, a zone in which non-visual related brain activity can be recorded. The aim of re-referencing is to remove the default brain activity, so that what is recorded in the channels of interest located in the occipital area is mainly due to the visual stimulus (Leuchs, 2019). This method has been effectively used in simultaneous EEG-fMRI studies because of the ease with which it can be attached to the scalp and because it favors the subsequent removal of artifacts during processing (Lei, 2017). To remove artifacts, the EEG signals were filtered. First, linear trends were removed, then a 3-Hz linear high-pass filter was applied, followed by the nonlinear Wavelet filter, and finally a 45-Hz linear low-pass filter was implemented. The nonlinear Wavelet filter used is a de-noising procedure, it was developed in three steps, all by performing 8 levels of decomposition ($N = 8$), having into account the db6 wavelet as the Wavelet family (Patil, 2012): The wavelet decomposition of the signal was calculated at level N, where the approximation and detail coefficients were obtained. Therefore, the threshold called universal was chosen and soft thresholding was applied to the detail coefficients. The value of the universal threshold is calculated with the Equation 1, where n is the number of samples of the signal (Guarnizo-Lemus, 2008).

$$\lambda = \sqrt{2\log(n)} \tag{1}$$

The soft thresholding is given by the Equation 2, were d_k^N is the wavelet detail coefficient k of level N, y sgn is the sign function (Guarnizo-Lemus, 2008).

$$d_k^N = \begin{cases} 0, & |d_k^N| < \lambda \\ \operatorname{sgn}\left(d_k^N\right)\left(|d_k^N - \lambda|\right), & |d_k^N| \geq \lambda \end{cases} \tag{2}$$

Finally, the wavelet reconstruction was computed from the original approximation coefficients of level N and the modified detail coefficients of levels 1 to N. Using this filter, it becomes possible to selectively retain coefficients surpassing a specified threshold for incorporation into the signal reconstruction. Meanwhile, coefficients falling below this threshold, regarded as signal noise, are discarded. This is due to the Wavelet transform's capability to concentrate the signal's energy within a handful of coefficients, whereas noise energy is distributed among numerous coefficients. As a result, the clean signal coefficients exhibit relatively higher values compared to those of the noise signal (Ballesteros Larrota, 2004). Subsequently, the non-filtered signal is subtracted from the Wavelet-filtered signal to account for the inherent lower amplitude of biological signals in relation to noise. For the linear filtering, FIR-type filters were used described by the Equation 3, where b_n are the coefficients of the filter and Z^{-1} correspond to the Z transform with M as the order of the filter. Finally, a 454-order high-pass filter and a 74-order low-pass filter were selected (Gunaydin, 2010).

$$y[n] = \sum_{n=0}^{M} b_n x[n] z^{-n} \tag{3}$$

For the frequency domain analysis, the Welch periodogram was used, which calculates the power spectral density (PSD) by applying the fast Fourier transform (Carvalho et al., 2015). Welch's method is performed by dividing the time signal into successive blocks, forming the periodogram for each block, and averaging. For the signal xxx, set mmm as the windowed, zero-padded frame. The signal is then defined as $x_m \triangleq w(n) \times (n + mR)$ for $n = 0, 1, \ldots, M1$ and $m = 0, 1, \ldots, K1$, where R is the window hop size, and K denotes the number of available frames. The Welch estimate of the power spectral density is given by Equation 4. The periodogram

Figure 4

Steps and Parameters of the Processing Pipeline for EEG Data

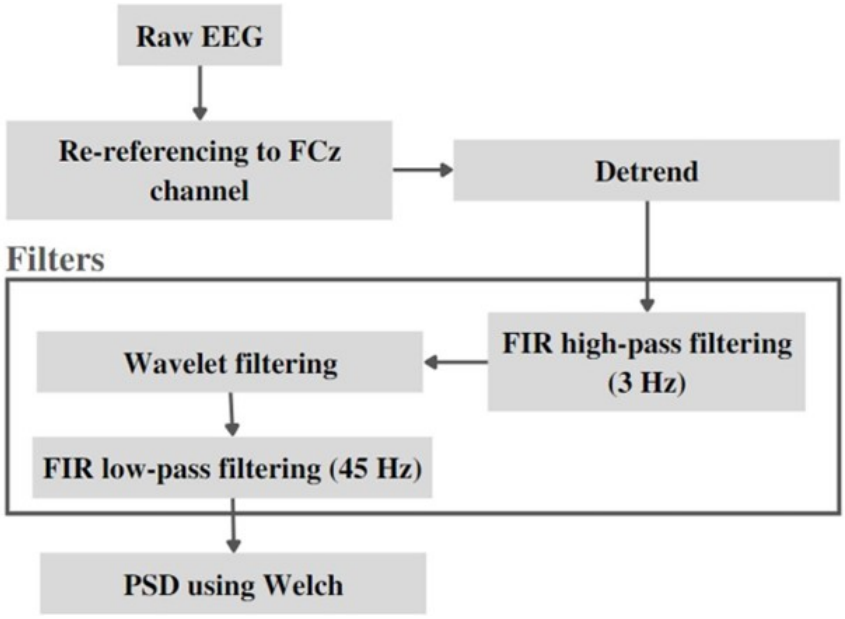

Note. This diagram shows the processing pipeline for EEG data, outlining the sequence of steps and the parameters used. The initial raw EEG data is first re-referenced to the FCz channel, which serves as a common reference point. Next, linear trends are removed (detrending) to minimize baseline drift. The data then undergoes high-pass filtering using a Finite Impulse Response (FIR) filter at a cutoff frequency of 3 Hz to remove low-frequency noise. After that, a wavelet-based filtering is applied to further denoise the signal. This is followed by a low-pass FIR filter with a cutoff frequency of 45 Hz to remove high-frequency artifacts. Finally, the Power Spectral Density (PSD) is calculated using the Welch method, providing a frequency-domain representation of the EEG signal. This pipeline aims to produce a cleaner signal for subsequent analysis and interpretation. Source: authors.

of the m block is given Equation 5 (Smith, 2011).

$$S_x^w[w_k] \triangleq \frac{1}{k} \sum_{M=0}^{k-1} P_{x_m,M(w_k)} \tag{4}$$

$$P_{x_m,M(w_k)} \triangleq \frac{1}{M} \left[\sum_{n=0}^{N-1} x_m[n] e^{\frac{-j2\pi nk}{N}} \right]^2 \tag{5}$$

To obtain the PSD with this method, a Hamming window was chosen with an overlap equal to the sampling frequency and length of each segment of 2 times the sampling frequency, obtaining values every .5 Hz.

2.5 Data Analysis

To establish the EEG signals recorded where VEP is presented, the signals to be analyzed were restricted to those recorded by the Oz electrode, since the area where this channel is located is closely associated with the activity of the primary visual cortex (Carvalho et al., 2015; Marcar, 2018). Likewise, two criteria were used to select the signals that comply with the SSVEP. First, the power spectral density at the stimulation frequency (5 Hz) had to be greater than the average of the density of the neighbouring frequencies (4 Hz and 6 Hz), meaning that the signal-to-noise ratio (SNR) had to be greater than 1, and, additionally, the power spectral density at the stimulation frequency had to be greater than both neighboring densities. Equation 6 represents the signal-to-noise ratio (Meigen, 1999):

$$s = \frac{m_j}{n_j} \tag{6}$$

$$n_j = \frac{m_{j-1} + m_{j+1}}{2} \tag{7}$$

Where: m_j: Magnitude of interest, n_j: Average magnitude of the two neighboring frequencies, corresponds to noise.

It is also verified that the frequency where the first harmonics are present fulfills the selection criteria.

A statistical analysis was conducted using the Wilcoxon signed-rank test to compare two related paired samples: one set corresponding to PSD measurements obtained while wearing glasses, and the other set corresponding to PSD measurements obtained without wearing glasses. The purpose of this analysis was to determine whether there were significant differences in PSD when observing a visual stimulus with and without glasses.

Figure 5

Effect of the Filtering Process on EEG Signals

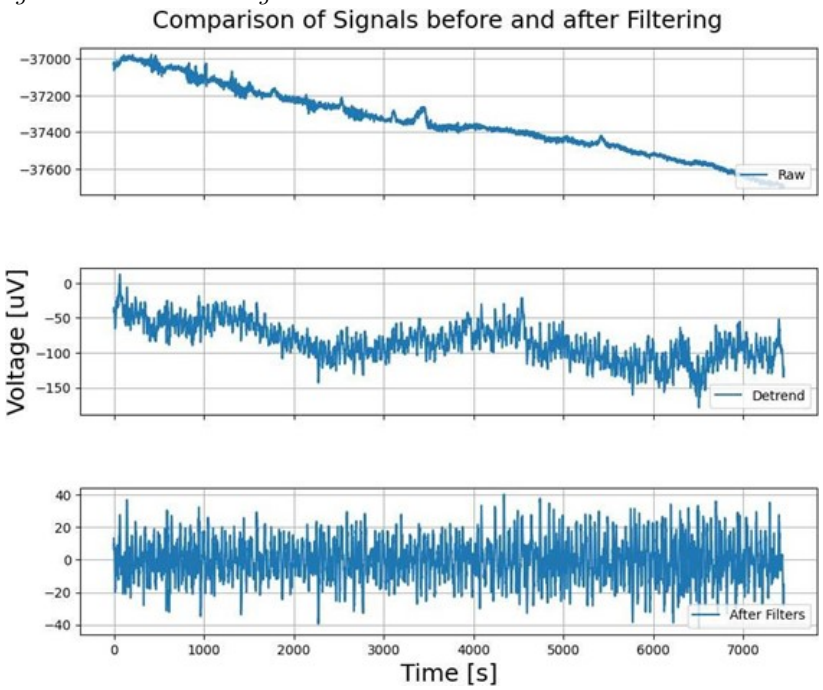

Note. This figure illustrates the effect of the filtering process on EEG signals. The top subplot shows the raw EEG signal before any processing. The middle subplot presents the signal after removing linear trends (detrending). The bottom subplot depicts the signal after applying both wavelet-based and FIR (Finite Impulse Response) filters, demonstrating a clearer signal with reduced noise. The x-axis represents time, while the y-axis indicates the amplitude of the EEG signal. Each subplot includes a grid for easier reference and a legend in the lower right corner to identify each stage of the filtering process. Source: authors.

It is important to note that while the statistical test involves a null hypothesis regarding the similarity of distributions between the paired samples (Woolson, 2008), in this context, our focus was on identifying and quantifying any observed differences, rather than testing a specific hypothesis. Thus, the analysis aimed to assess the magnitude of the differences between the two conditions and determine their statistical significance.

This test was performed using the SciPy library in Python, and the significance level considered was .05.

2.6 Survey

User comfort was related to the performance of the representative visual stimuli. This was measured subjectively by a three-question survey administered to each participant at the end of each experiment. The survey questions were:

- Please rate your comfort level during the procedure using the following options: Very comfortable, Comfortable, Normal, Increasing discomfort over time.
- How well were you able to see the changes in the images presented, from the largest to the smallest?
- Comments and suggestions.

The purpose of this survey was to assess the comfort level of patients during the enrolment process, with the goal of effectively presenting the portable capture device as a viable option that would be well received by participants.

3. Results

After the recording of the signals, the described preprocessing pipeline was applied. The change in the signal of one of the subjects recorded after performing the filtering process selected for the present study can be seen in Figure 5 . The first graph corresponds to the unfiltered signal, the second one, to the signal after eliminating linear trends, and the last one, the signal after applying the FIR filters and Wavelet de-noising.

After the acquisition and processing of the signals, these were analyzed in the frequency domain, expecting neural activation at the stimulation frequencies (SSVEP). Figure 6 shows the comparison of the PSD obtained for the subjects when observing the stimulus with and without glasses. The values obtained for subjects with glasses and without them was 2.60±0.57 SNR and 2.17±.75 SNR, respectively. Neural activation on the stimulation frequency was achieved in both cases with significant differences in amplitude (30 PSD).

Figure 6

Comparison of the Average Power Spectral Density (PSD) for the two Subjects

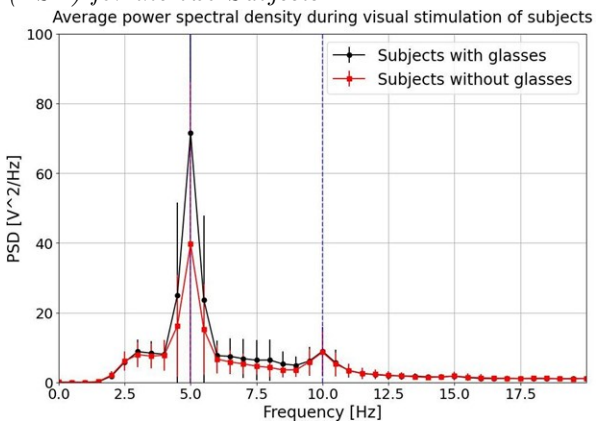

Note. This graph presents a comparison of the average power spectral density (PSD) at 5 Hz obtained during LogMAR 1.18 stimulation for two groups of subjects: those wearing glasses and those not wearing glasses. The x-axis represents frequency in Hz, while the y-axis indicates the PSD. The black curve represents the average PSD for subjects wearing glasses, while the red curve represents the average for those not wearing glasses. Error bars depict the standard deviation for each group. Dashed blue vertical lines at 10 Hz and 20 Hz serve as reference markers. This plot visualizes differences in PSD between the two groups, suggesting variations in visual processing depending on the presence or absence of glasses. Source: authors.

During this comparison, a paired non-parametric Wilcoxon test was conducted with the null hypothesis, assuming that both groups originated from the same distribution. The obtained p-value of .03 indicated statistically significant differences, suggesting distinct behaviors in PSD when subjects wore and did not wear glasses. This signifies differences in visual perception with and without glasses, as supported by Figure 6, which demonstrates increased visual perception in subjects when wearing glasses.

It is important to highlight that that not all subjects had identical visual disorders prompting the use of glasses. However, given the aim of comparing general differences in visual perception (assessed through PSD response) when wearing versus not wearing glasses, the diverse range of visual disorders or impairments among participants facilitated the observation of the intended phenomena. Furthermore, all findings indicated a reduction in the amplitude of neural response at the stimulation frequency, as expected due to decreased visual perception when not wearing glasses, despite the presence of varying visual disorders.

To compare EEG at rest and during stimulation, Figure 7 shows the average power spectral density during a eyes-open resting state and stimulation state, where both present a different behavior, mainly around the stimulation frequency (5 Hz), indicating changes in the neural activity due to the visual stimulation used.

Figure 7

Comparison of Average Spectral Density Obtained during Visual Stimulation

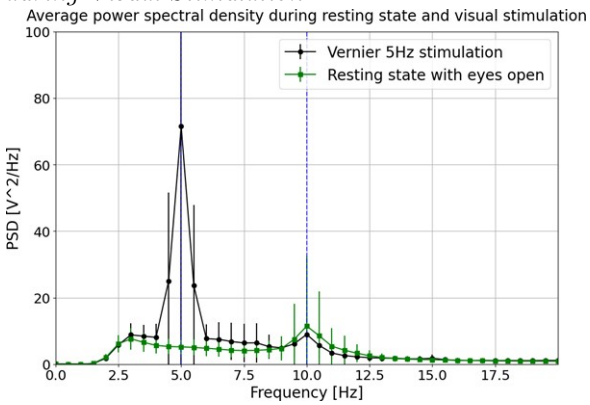

Note. It was used a Vernier pattern at 5 Hz, as part of LogMAR 1.18 stimulation, and during the eyes-open resting state. Error bars represent the standard deviation. Dashed blue vertical lines at 10 Hz and 20 Hz serve as reference markers. Source: authors.

Bar plots were implemented to identify subject-level differences (see Figure 8). It shows that 90.5% of subjects have more neural activation using glasses than without glasses, and it could be explained by the correction of the visual acuity of the glasses. Additionally, there are two atypical values (Subjects 8 and 17, account for the variability observed in the power spectral density plots).

The results of the satisfaction survey showed how the subjects felt during the procedure, as illustrated in Figure 9. The results of the survey indicate that 42% of the subjects reported feeling comfortable during the registration process, while 37% mentioned feeling very comfortable. A smaller percentage, 12%, expressed a neutral perception of their comfort level, describing it as “Normal”. Finally, only 9% of the participants reported an increase in discomfort over time throughout the registration procedure, according to the survey responses. Likewise, most of the respondents had no suggestions or comments.

4. Discussion

This study successfully demonstrated the feasibility of acquiring, processing, and analyzing EEG signals of the visual system using a transferable EEG device. The cost-effectiveness of OpenBCI, which is at least three times cheaper compared to traditional EEG devices, highlights the potential for developing affordable solutions in the field of EEG acquisition and analysis (Bach, 2019; Hemptinne et al., 2019; Kiiski et al., 2016; Sahel et al., 2021; Sarzaeim et al., 2022; Zheng et al., 2019). The exper-

Figure 8

Power Spectral Density (PSD) during 5 Hz Frequency Simulation for the two Groups

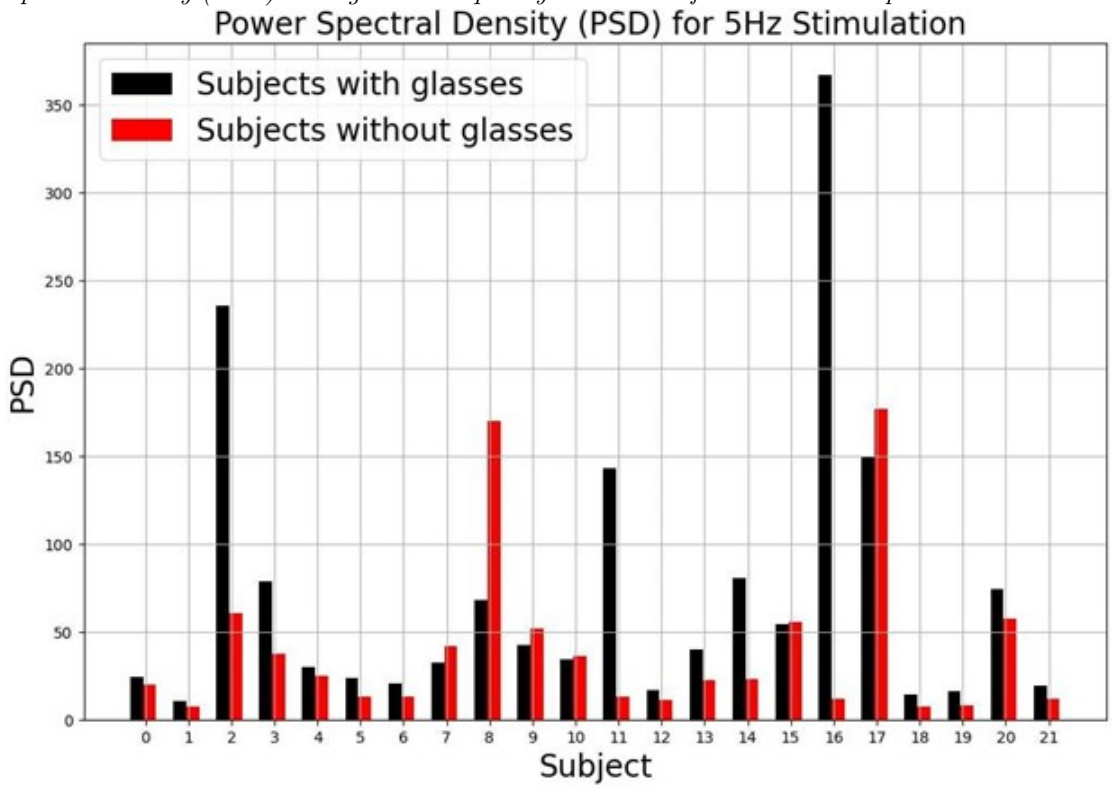

Note. Bar plot showing Power Spectral Density (PSD) during 5 Hz frequency stimulation for two groups: subjects with glasses (black bars) and subjects without glasses (red bars). The x-axis represents different subjects, and the y-axis indicates the PSD in the measured units. Source: authors.

Figure 9

Distribution of Subjects' Comfort Levels during the Test

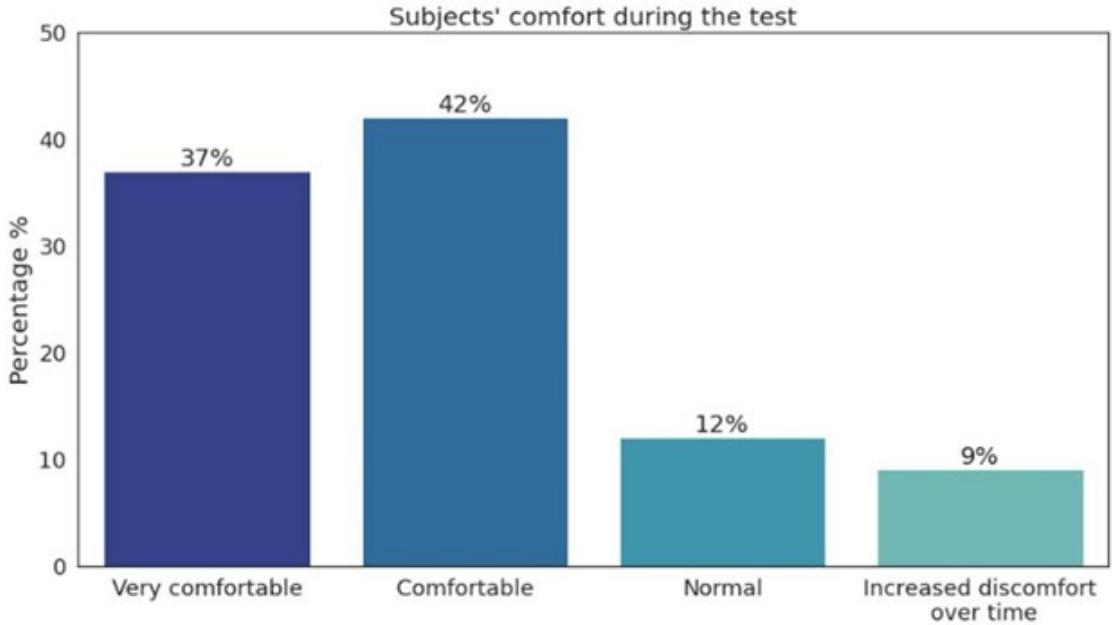

Note. 37% reported feeling "Very comfortable", 42% reported feeling "Comfortable", 12% reported feeling "Normal", and 9% reported experiencing increased discomfort over time. Source: authors.

imental setup utilizing OpenBCI as the portable EEG equipment proved to be suitable for clinical office implementation, as it does not require significant space and the overall cost is approximately 1060 USD, including the OpenBCI device, electrodes, electrode cap gel, and the display. The study employed specific visual stimuli, such as the Vernier stimulus, which are well-documented in the literature and known for eliciting steady-state visual evoked potentials (Tan et al., 2018; Zheng et al., 2020). Care was taken to ensure adequate stimulation times to prevent visual fatigue and enhance comfort for the subjects participating in the tests. This comfort is reflected in the results of the survey carried out, where more than 70% of the subjects expressed feeling comfortable or very comfortable during the registration. The perception results were taken with a subject approach and for future evaluations of the data. In the short term, this study seeks to characterize the ability of the experiment to capture the SSVEP. However, in the long term it, it is proposed to implement a system like this for therapy inside or outside a doctor's office, and the possibility of extending this stimulus in applications involving measure visual acuity. The results of the study demonstrated excellent visual activation in response to the Vernier acuity stimulus at 5 Hz for the LogMAR 1.18. The signal-to-noise ratio (SNR) values were 2.59±.57 SNR and 2.17±.75 SNR for subjects with and without glasses, respectively, indicating the potential improvement in neural activation through visual acuity correction. Regarding the stimulation equipment, certain factors that could introduce variability in the results were identified. These factors included the precision and accuracy of the equipment to present stimuli at the desired frequency, potential participant movements during stimulation, inherent noise from participants' signals, and visual fatigue from prolonged screen observation. The goal in this type of studies is to reduce complexity, cost, and difficulty by utilizing open-source or commercial BCI software, which enables adaptability to different experimental situations and facilitates the operation of entire research programs. Low-cost EEG headsets offer portability and varying degrees of success for real-world occupational use, but open-source software and contextual development can enhance their potential. By leveraging open components and collaborative development, the BCI community aims to extend this technology to the general population and develop stable, scalable applications comparable to medical-grade equipment (Chandran, 2020). In conclusion, this study contributes to the development of cost-effective and portable EEG solutions for visual system analysis. It demonstrates the potential for applying transferable EEG devices in clinical settings and highlights the importance of tailored visual stimuli for reliable neural activation (Tan et al., 2018; Zheng et al., 2020).

5. Conclusions

The conclusions of the study underscore its valuable contribution to advancing cost-effective and portable EEG solutions for the analysis of the visual system. Notably, the research illustrates the feasibility of employing transferable EEG devices in clinical settings, emphasizing the significance of customized visual stimuli to ensure consistent neural activation.

The findings emphasize the potential of low-cost EEG in terms of portability, while acknowledging varying degrees of success in real-world occupational applications. The study suggests that the optimization of these devices can be achieved through the utilization of open-source software and contextual development, thereby enhancing their overall capabilities. The collaborative efforts within the Brain-Computer Interface (BCI) community, focusing on open components and shared development, emerge as a promising avenue.

Future works in this field should concentrate on refining the performance of low-cost EEG through continued collaborative efforts. Additionally, exploring diverse visual stimuli and their impact on neural responses could further enhance the reliability and applicability of these devices. Further research could delve into the development of user-friendly interfaces and the integration of advanced signal processing techniques to elevate the overall effectiveness and accessibility of cost-effective EEG solutions. These endeavors will play a pivotal role in bridging the gap between affordable EEG technology and its widespread utilization in both clinical and occupational settings.

6. Acknowledgments

This research was developed thanks to funding from the "Fundación para la Promoción de la Investigación y la Tecnología del Banco de la República", of the project "Platform for the evaluation of visual physiology base on low cost and portable electroencephalography" with code 4.418. Finally, we would like to thank all the volunteers who participated in the tests for their willingness and time.

References

Almoqbel, F. M., Irving, E. L., & Leat, S. J. (2017). Visual Acuity and Contrast Sensitivity Development in Children: Sweep Visually Evoked Potential and Psychophysics. *Optometry and vision science*, *94*(8), 830–837. https://doi.org/10.1097/OPX.0000000000001101

Alouani, A. T., & Elfouly, T. (2022). Traumatic Brain Injury (TBI) Detection: Past, Present, and Future. *Biomedicines*, *10*(10), 2472. https://doi.org/10.3390/biomedicines10102472

Bach, M., & Heinrich, S. (2019). Acuity VEP: improved with machine learning. *Doc. Ophthalmol*, *139*(2), 113–122. https://doi.org/10.1007/s10633-019-09701-x

Baker, D. H., Simard, M., Saint-Amour, D., & Hess, R. F. (2015). Steady-State Contrast Response Functions Provide a Sensitive and Objective Index of Amblyopic Deficits. *Investigative Ophthalmology Visual Science*, *56*(2), 1208. https://doi.org/10.1167/IOVS.14-15611

Ballesteros Larrota, D. M. (2004). Aplicación de la transformada wavelet discreta en el filtrado de señales bioeléctricas. *Umbral Científico*, *5*, 92–98.

Beniczky, S., & Schomer, D. L. (2020). Electroencephalography: Basic biophysical and technological aspects important for clinical applications. *Epileptic Disorders*, *22*(6), 697–715. https://doi.org/10.1684/epd.2020.1217

Brienza, M., & Mecarelli, O. (2019). Neurophysiological Basis of EEG BT. In O. Mecarelli (Ed.), *Clinical electroencephalography* (pp. 9–21). Springer International Publishing. https://doi.org/10.1007/978-3-030-04573-9_2

Cadavid, V., Salas, E., Gonzalez, S., Henao, V., Ortega, D., Suarez, J. C., & Ochoa, J. (2021). Captura y análisis de potenciales visuales en estado estacionario usando tecnología portable y de bajo costo. *22nd Symposium on Image, Signal Processing and Artificial Vision, STSIVA 2021 – Conference Proceedings*. https://doi.org/10.1109/STSIVA53688.2021.9592014

Carvalho, S. N., Costa, T. B., Uribe, L. F., Soriano, D. C., Yared, G. F., Coradine, L. C., & Attux, R. (2015). Comparative analysis of strategies for feature extraction and classification in SSVEP BCIs. *Biomedical Signal Processing and Control*, *21*, 34–42. https://doi.org/10.1016/J.BSPC.2015.05.008

Chandran, K. S., & Kiruba Angeline, T. (2020). Identification of disease symptoms using taste disorders in electroencephalogram signal. *Journal of Computational and Theoretical Nanoscience*, *17*(5), 2051–2056.

Fox, M., Barber, C., Keating, D., & Perkins, A. (2014). Comparison of cathode ray tube and liquid crystal display stimulators for use in multifocal VEP. *Documenta ophthalmologica. Advances in ophthalmology*, *129*(2), 115–122. https://doi.org/10.1007/S10633-014-9451-0

Guarnizo-Lemus, C. (2008). Análisis de reducción de ruido en señales eeg orientado al reconocimiento de patrones. *TecnoLógicas*, *21*, 67–80. https://doi.org/10.22430/22565337.248

Gunaydin, O., & Ozkan, M. (2010). Design of a Brain Computer Interface system based on electroencephalogra (EEG). *4th European Education and Research Conference (EDERC 2010)*.

Hemptinne, C., Liu-Shuang, J., Yuksel, D., & Rossion, B. (2019). Rapid Objective Assessment of Contrast Sensitivity and Visual Acuity with Sweep Visual Evoked Potentials and an Extended Electrode Array. *Journal of Vision*, *19*(8), 87. https://doi.org/10.1167/19.8.87

Kadri, A., & Apriani, N. (2022). Electroencephalography Findings in Traumatic Brain Injury. *The Open Neurology Journal*, *16*(1), 1–11. https://doi.org/10.2174/1874205x-v16-e2206100

Kiiski, H. S., Riada, S. N., Lalor, E. C., Gonçalves, N. R., Nolan, H., Whelan, R., Lonergan, R., Kelly, S., O'Brien, M. C., Kinsella, K., Bramham, J., Burke, T., Donnchadha, Ó., S., H., M., T., N., & Reilly, R. B. (2016). Delayed P100-Like Latencies in Multiple Sclerosis: A Preliminary Investigation Using Visual Evoked Spread Spectrum Analysis. *PloS one*, *11*(1). https://doi.org/10.1371/JOURNAL.PONE.0146084

Lantz, C. L., & Quinlan, E. M. (2021). High-Frequency Visual Stimulation Primes Gamma Oscillations for Visually Evoked Phase Reset and Enhances Spatial Acuity. *Cerebral cortex communications*, *2*(2), tgab016. https://doi.org/10.1093/texcom/tgab016

Lei, X., & Liao, K. (2017). Understanding the Influences of EEG Reference: A Large-Scale Brain Network Perspective. *Front. Neurosci*, *11*. https://doi.org/10.3389/fnins.2017.00205

Leuchs, L. (2019, May 3). *Choosing your reference - and why it matters*. Brain Products Press Release. https://pressrelease.brainproducts.com/referencing/

Marcar, V. L., & Jäncke, L. (2018). Stimuli to differentiate the neural response at successive stages of visual processing using the vep from human visual cortex. *Journal of neuroscience methods*, *293*, 199–209. https://doi.org/10.1016/J.JNEUMETH.2017.09.015

Meigen, T., & Bach, M. (1999). On the statistical significance of electrophysiological steady-state responses. *Documenta ophthalmologica. Advances in ophthalmology*, *98*(3), 207–232. https://doi.org/10.1023/A:1002097208337

Mora-Cortes, A., Ridderinkhof, K. R., & Cohen, M. X. (2018). Evaluating the feasibility of the steady-state visual evoked potential (SSVEP) to study temporal attention. *Psychophysiology*, *55*(5). https://doi.org/10.1111/PSYP.13029

Nicolas-Alonso, L. F., & Gomez-Gil, J. (2012). Brain computer interfaces, a review. *Sensors*, *12*(2), 1211–1279. https://doi.org/10.3390/s120201211

Norcia, A. M., Appelbaum, L. G., Ales, J. M., Cottereau, B. R., & Rossion, B. (2015). The steady-state

visual evoked potential in vision research: A review. *Journal of Vision*, *5*, 4. https://doi.org/10.1167/15.6.4

Nuwer, M. R. (2018). 10-10 electrode system for EEG recording. *Clinical Neurophysiology*, *129*(5), 1103. https://doi.org/10.1016/j.clinph.2018.01.065

O'Hare, L. (2017). Steady-state VEP responses to uncomfortable stimuli. *European Journal of Neuroscience*, *45*(3), 410–422. https://doi.org/10.1111/EJN.13479

Orban, M., Elsamanty, M., Guo, K., Zhang, S., & Yang, H. (2022). A Review of Brain Activity and EEG-Based BrainComputer Interfaces for Rehabilitation Application. *Bioengineering*, *9*(12). https://doi.org/10.3390/bioengineering9120768

Ortega, D., Henao, V., & Ochoa, J. (2019). Ssvep study in monocular and binocular vision. *2019 XXII Symposium on Image, Signal Processing and Artificial Vision (STSIVA)*. https://doi.org/10.1109/STSIVA.2019.8730241

Patil, P. B., & Chavan, M. S. (2012). A wavelet based method for denoising of biomedical signal. *International Conference on Pattern Recognition, Informatics and Medical Engineering*, 278–283. https://doi.org/10.1109/ICPRIME.2012.6208358

Richard, B., Chadnova, E., & Baker, D. H. (2018). Binocular vision adaptively suppresses delayed monocular signals. *NeuroImage*, *172*, 753–765. https://doi.org/10.1016/J.NEUROIMAGE.2018.02.021

Sahel, J. A., Boulanger-Scemama, E., Pagot, C., Arleo, A., Galluppi, F., Martel, J. N., & Roska, B. (2021). Partial recovery of visual function in a blind patient after optogenetic therapy. *Nature Medicine*, *27*(7), 1223–1229. https://doi.org/10.1038/s41591-021-01351-4

Sanchez-Lopez, J., Pedersini, C. A., Russo, F., Cardobi, N., Fonte, C., Varalta, V., Prior, M., Smania, N., Savazzi, S., & Marzi, C. A. (2019). Visually evoked responses from the blind field of hemianopic patients. *Neuropsychologia*, *128*, 127–139. https://doi.org/10.1016/J.NEUROPSYCHOLOGIA.2017.10.008

Sarzaeim, F., Hashemzehi, M., Mohammad Masoud Shushtarian, S., Shojaei, A., & Naghib, J. (2022). Flash visual evoked potential as a suitable technique to evaluate the extent of injury to visual pathway following head trauma. *Journal of Ophthalmology and Research*, *05*(01), 20–23. https://doi.org/10.26502/fjor.2644-00240053

Smith, J. O. (2011). Spectral Audio Signal Processing. In *Center for computer research in music and acoustics (ccrma)* (pp. 1–674.)

Tan, Y., Tong, X., Chen, W., Weng, X., He, S., & Zhao, J. (2018). Vernier But Not Grating Acuity Contributes to an Early Stage of Visual Word Processing. *Neuroscience Bulletin*, *34*(3), 517–526. https://doi.org/10.1007/s12264-018-0220-z

Woolson, R. F. (2008). Wilcoxon Signed-Rank Test. *Wiley Encyclopedia of Clinical Trials*, 1–3. https://doi.org/10.1002/9780471462422.EOCT979

Zheng, X., Xu, G., Wang, Y., & Han, C. (2019). Objective and quantitative assessment of visual acuity and contrast sensitivity based on steady-state motion visual evoked potentials using concentric-ring paradigm. *Documenta Ophthalmologica*, *139*. https://doi.org/10.1007/s10633-019-09702-w

Zheng, X., Xu, G., Zhang, K., & Liang, R. (2020). Assessment of Human Visual Acuity Using Visual Evoked Potential. *A Review. Sensors (Basel)*, *20*(19). https://doi.org/10.3390/s20195542

Zhong, Y., Wei, H., Chen, L., & Wu, T. (2023). Automated EEG Pathology Detection Based on Significant Feature Extraction and Selection. *Mathematics*, *11*, 1619. https://doi.org/10.3390/math11071619